Plasmonics
https://doi.org/10.1007/s11468-023-01945-3

RESEARCH

Improved Surface Plasmon Effect in Ag-based SPR Biosensor with Graphene and WS_2: An Approach Towards Low Cost Urine-Glucose Detection

Archana Yadav[1] · Madhusudan Mishra[2] · Sukanta K. Tripathy[2] · Anil Kumar[3] · O. P. Singh[3] · Preeta Sharan[4]

Received: 16 June 2023 / Accepted: 6 July 2023

Abstract
Gold and silver are the two notable noble metals with wide implications in surface plasmon resonance (SPR) based sensors. Gold possesses a superior SPR phenomenon compared to silver, however, with extremely high costs. To resolve this problem, the current study proposes a new gold–free SPR biosensor design employing silver as the noble metal for efficient detection of blood glucose using urine as the biosample. The proposed design employs two types of 2D materials such as graphene and tungsten disulfide (WS_2) to enhance the sensitivity of the silver-based SPR biosensor. An investigation for design of a low-cost biosensor for urine-glucose detection is done using the proposed configuration. The glucose concentration in the biosample ranges from 0 to 15 mg/dl (for normal persons) and 0.625 gm/dL, 1.25 gm/dL, 2.5 gm/dL, 5 gm/dL, and 10 gm/dL (for diabetic persons), with corresponding refractive indices of 1.335, 1.336, 1.337, 1.338, 1.341, and 1.347. The material's type, order, and thickness have been chosen through numerous case studies. It is worth noting that, with 4-layer graphene (0.34 nm) and 4-layer WS_2 (0.8 nm), the proposed silver-based SPR biosensor shows improved sensitivity (288.86°/RIU) and figure of merit (88.89/RIU) than its gold-based counterpart (sensitivity 150°/RIU). Finally, this study is also compared with similar reported literatures. The proposed structure has potential to develop low-cost and efficient SPR-based biosensors (glucose sensors), with a substantial shift in resonance angle of SPR curves as shown in the present study.

Keywords Surface plasmons · Biosensor · Refractive index · Kretschmann configuration · Graphene · WS_2 · Reflectance · Gold free · Highly sensitive

Introduction

Among the many pervasive and incurable diseases of the present era of high-tech lifestyles, diabetes is the one that is currently the leading health concern on a global scale. Affecting an estimated 500 million individuals worldwide, the disease is still spiralling [1]. Diabetes is also becoming a concern at the paediatric level [2]. Though all types of diabetes are not curable, it is possible to bring them under control through regular testing and treatment. Nonetheless, invasive methods are still widely used for the detection of blood glucose levels, including both lab-grade and kit-based (domiciliary) testing [3]. However, it is a painful process, which sometimes put patients (especially children) into panic for frequent testing, [4]. This leads to improper detection and diagnosis of diabetes and rises the daily patient volume. Therefore, there is always a strong need for developing non-invasive blood-glucose testing techniques with low cost, to promote frequent testing among the patients irrespective of their age group and financial status [5].

Recently, surface plasmon resonance-based sensors have drawn potential research interest in biomedical and other applications [6, 7]. Triggered by the coupling of photons and electrons, they are linked to the interactions of electromagnetic waves at the metal and dielectric interface [8, 9]. At

✉ Madhusudan Mishra
madhusudandbt@gmail.com

[1] Department of ECE, Integral University, Lucknow 226026, India

[2] Centre of Excellence in Nano Science and Technology for development of Sensors, Berhampur University, Berhampur 760007, Odisha, India

[3] Department of ECE, ASET, Amity University, Lucknow Campus, 226010 Lucknow, UP, India

[4] Department of ECE, The Oxford College of Engineering, Bengaluru 560068, India

Published online: 15 July 2023

resonance, the energy and momentum of the incident light (p-polarized) are preserved, and the reflectance becomes minimal due to the maximum excitation of the surface plasmons [10, 11]. At this point, the incident wave vector becomes equal to the plasmons' propagation constant. This can be demonstrated using Eq. (1) given below [12].

$$k_i = k_p \tag{1}$$

where $k_i = \frac{\omega}{c} n_1 \sin\theta_i$, and

$$k_p = \frac{\omega}{c}\sqrt{\frac{\epsilon_m \epsilon_d}{\epsilon_m + \epsilon_d}}$$

ϵ_m and ϵ_d are the permittivity constant of metal and dielectric respectively and n_1 is the refractive index of the first layer.

Gold and silver are the most commonly used metals for design of SPR based sensors, where the former one offers better sensitivity [9]. However, the high cost of gold yields the quest for developing a gold free and efficient SPR based sensor [7].

Two-dimensional materials such as graphene and WS_2 are becoming popular for enhancing the SPR effect [13]. Unlike the conventional noble metals, graphene can create surface plasmon polaritons (SPPs) at frequencies in the mid-infrared to terahertz range. Moreover, the confinement volume of such SPPs is substantially less, and their lifespan is much longer than that of metals. Several works using graphene in innovative plasmonic sensors have already been reported [8]. WS_2, often compared to graphene, has a hexagonal crystal structure made up of S-W-S monolayers that are covalently bonded to one another and stacked by weak van der Waals forces [14]. As a result, WS_2 is also recognised as a promising 2D layered nanomaterial [15]. With its high surface-to-volume ratio and layer-dependent electronic and optical properties, large photoresponsivity, high density of electronic states, large band gaps in the visible to near-infrared spectrum, and strong photoluminescence, WS_2 is a typical type of two-dimensional transition metal dichalcogenides (TMDCs) material that offers numerous opportunities in the development of new biological and chemical sensors.

To avoid the excessive cost of gold, an SPR sensor for urine-glucose detection is developed in this work, employing silver as the metal layer, along with graphene and WS_2. About twice as sensitive as a fundamental Au-based device design, the proposed sensor achieves a sensitivity and figure of merit of 288.86°/RIU and 88.89/RIU respectively.

Section "Device Structure" of this manuscript gives a detailed explanation on the device structure, and in Section "Theory", a broad overview of the theory is given. Section "Numerical Results" contains the findings of the whole work as well as an analysis of those findings, followed by the fabrication feasibility of the proposed structure given in Section "Fabrication Feasibility". Section "Conclusions" gives the conclusion of the whole work.

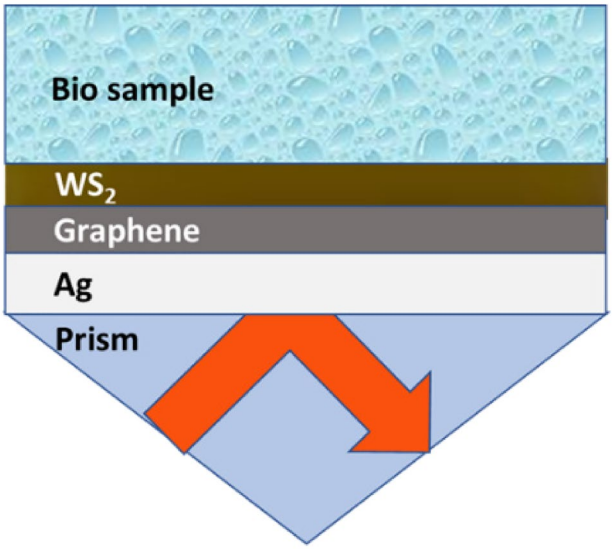

Fig. 1 Schematic of the proposed Graphene-WS_2 based five layered SPR biosensor structure

Device Structure

The proposed biosensor is schematically depicted in Fig. 1. It is a five-layered Kretschmann configuration comprising a prism, silver, graphene, tungsten disulfide, and biosample. Considering the necessity to match the momentum of light, the prism is made of BK-7 glass and is the first layer of the structure. The prism's refractive index (n_{prism}) is taken to be 1.515, which could be computed using Eq. (2) [9].

$$n_{prism} = \left(1 + \frac{1.03961212\,\lambda^2}{\lambda^2 - 0.00600069867} + \frac{1.01046945\,\lambda^2}{\lambda^2 - 103.560653} + \frac{0.231792344\,\lambda^2}{\lambda^2 - 0.0200179144}\right)^{1/2} \tag{2}$$

where λ represents the wavelength of the incident light.

The Ag layer is deposited on the base of the prism, and its refractive index is calculated by the Drude–Lorentz model [11].

$$n_{Ag} = \left(1 - \frac{\lambda^2 * \lambda_c}{\lambda_p^2(\lambda_c + \lambda * i)}\right)^{1/2} \tag{3}$$

where, λ is the wavelength of incident light. λ_p(plasmon wavelength) and λ_c (collision wavelength) for Ag are 1.4541×10^{-7} m and 1.7614×10^{-5} m respectively [12].

Further, Table 1 shows refractive indices for the graphene and WS_2 layers; the third and fourth layers of the proposed structure. The structure's final layer is urine (biosample) and its refractive indices are taken as 1.335, 1.336, 1.337, 1.338, 1.341, and 1.347 for corresponding glucose concentrations of 0 g/dL, 0.625 g/dL, 1.25 g/dL, 2.5 g/dL, 5 g/dL, and 10 g/dL, respectively [16].

Table 1 Values of Refractive Indices for 2D materials

2 D Materials	Monolayer Thickness	Refractive Index	Ref.
Graphene	0.34 nm	3.5 + 0.01i	[17]
WS_2	0.80 nm	4.8937 + 0.3123i	[18]

Theory

When light is incident on the proposed five-layered structure, reflection occurs at each interface. To determine the total reflection intensity of the entire structure, collective reflection has been taken into account [19]. For this, if a propagating wave is moving from medium k towards the medium $k+1$, then it's operational principle can be defined by the transfer matrix method as defined by Eq. (4) [20].

$$M_k = \begin{bmatrix} \cos\beta_k & -\sin\beta_k/q_k \\ -iq_k\sin\beta_k & \cos\beta_k \end{bmatrix} \tag{4}$$

where, k denotes an arbitrary number, β_k denotes phase constant, and q_k denotes the refractive indices of the corresponding layers. Further, phase constant can be defined as [11]:

$$\beta_k = \frac{2\pi}{\lambda} d_{prism}\sqrt{n_{prism}^2 - \left(n_{prism}\sin\theta\right)}, \text{ and} \tag{5}$$

$$q_k = \frac{\sqrt{n_k^2 - (n_{prism}\sin\theta)^2}}{n_k^2} \tag{6}$$

where n_k is the refractive index of respective layer and θ is the incident angle. The total transfer matrix of the multilayer structure can be calculated by using a transfer matrix M_{total} for every monolayer which is as follows [21].

$$M_{total} = \Pi_{k=2}^{m-1} = \begin{bmatrix} m_{11} & m_{12} \\ m_{21} & m_{22} \end{bmatrix} \tag{7}$$

Total reflection coefficient r, for multilayer structure can be defined as [21]

$$r = \frac{(m_{11} + m_{12}q_n)q_1 - (m_{21} + m_{22}q_n)}{(m_{11} + m_{12}q_n)q_1 + (m_{21} + m_{22}q_n)} \tag{8}$$

On further solving, total reflectance can be represented as R, where

$$R = |r|^2 \tag{9}$$

Additionally, the sensitivity of the biosensor can be defined as follows [22]

$$S = \frac{\Delta\theta_{res}}{\Delta n_s} \tag{10}$$

where, $\Delta\theta_{res}$ represents the difference in resonance angle and Δn_s is the difference in the refractive index of the biosample. Moreover, the figure of merit of biosensor can be defined as the ratio of its sensitivity to the full width at half maximum (FWHM) of its reflectance curve [20].

$$FoM = \frac{S}{FWHM} \tag{11}$$

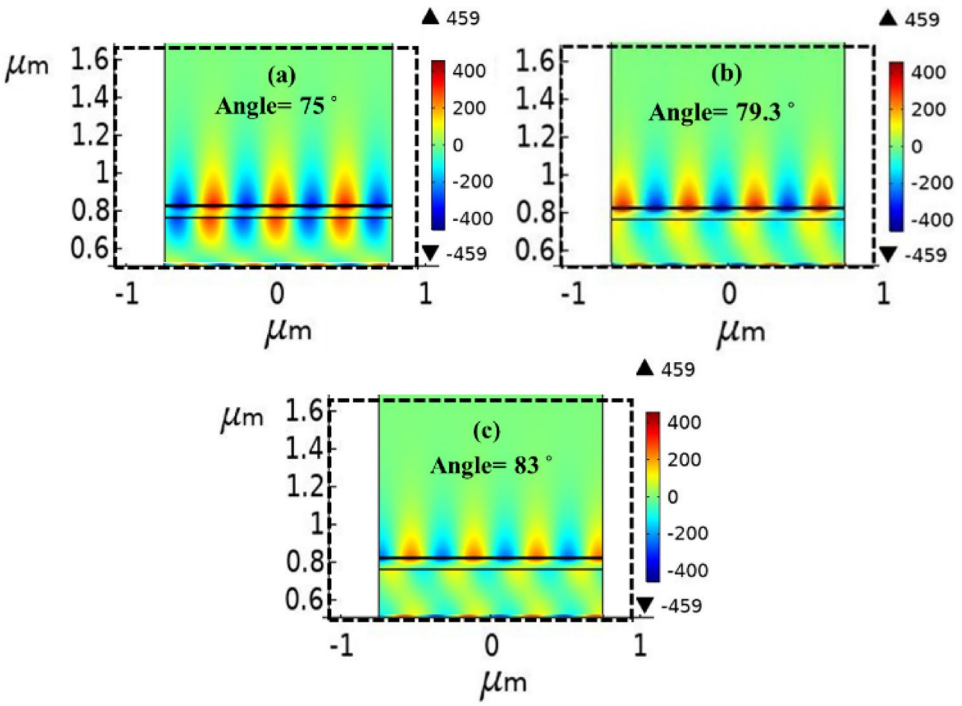

Fig. 2 Plasmonic excitation state for the proposed structure for **a**. $\theta = 75^o$, **b**. $\theta = 79.3^o$ and **c**. $\theta = 83^o$ (angle of resonance)

Numerical Results

The numerical study of the proposed structure is done using the finite element method-based simulation tool COMSOL. To perform the simulation, the physics of electromagnetic waves in the frequency domain is utilized. We have used a maximum growth rate of 1.1 and the maximum element size of 0.0457 m for the meshing process. The minimum element size has been set at 9.13e-5 m. In addition, we have utilized a free triangular mesh with distribution at each layer's interfaces, considering there are approximately 200 elements.

Various solutions of urine glucose concentrations that provide refractive indices of 1.335, 1.36, 1.337, 1.338, 1.341, and 1.347 are considered as the biosample. Plasmonic excitation state for the simulated structure prism/Ag/graphene/WS_2/biosample for the resonance angle at $\theta = 75^o$, $\theta = 79.3^o$ and $\theta = 83^o$ is depicted in Fig. 2. It can be seen that, the plasmon waves show resonance at $\theta = 79.3^o$.

Optimization of the proposed biosensor is done by optimising the thickness of the metal, graphene, and WS_2 layers. First, an investigation has been carried out to determine the optimum thickness of the Ag layer, deposited on the base of the prism. To accomplish this, it is vital to locate the lowest minimum reflectance point (R_{min}), as shown in Fig. 3a, as R_{min} ensures the maximum excitation state of surface plasmons in the proposed structure. The optimized thickness of the Ag layer can be taken as 56 nm, as it can be noted from Fig. 3a. The value of R_{min} for 56 nm of Ag thickness is

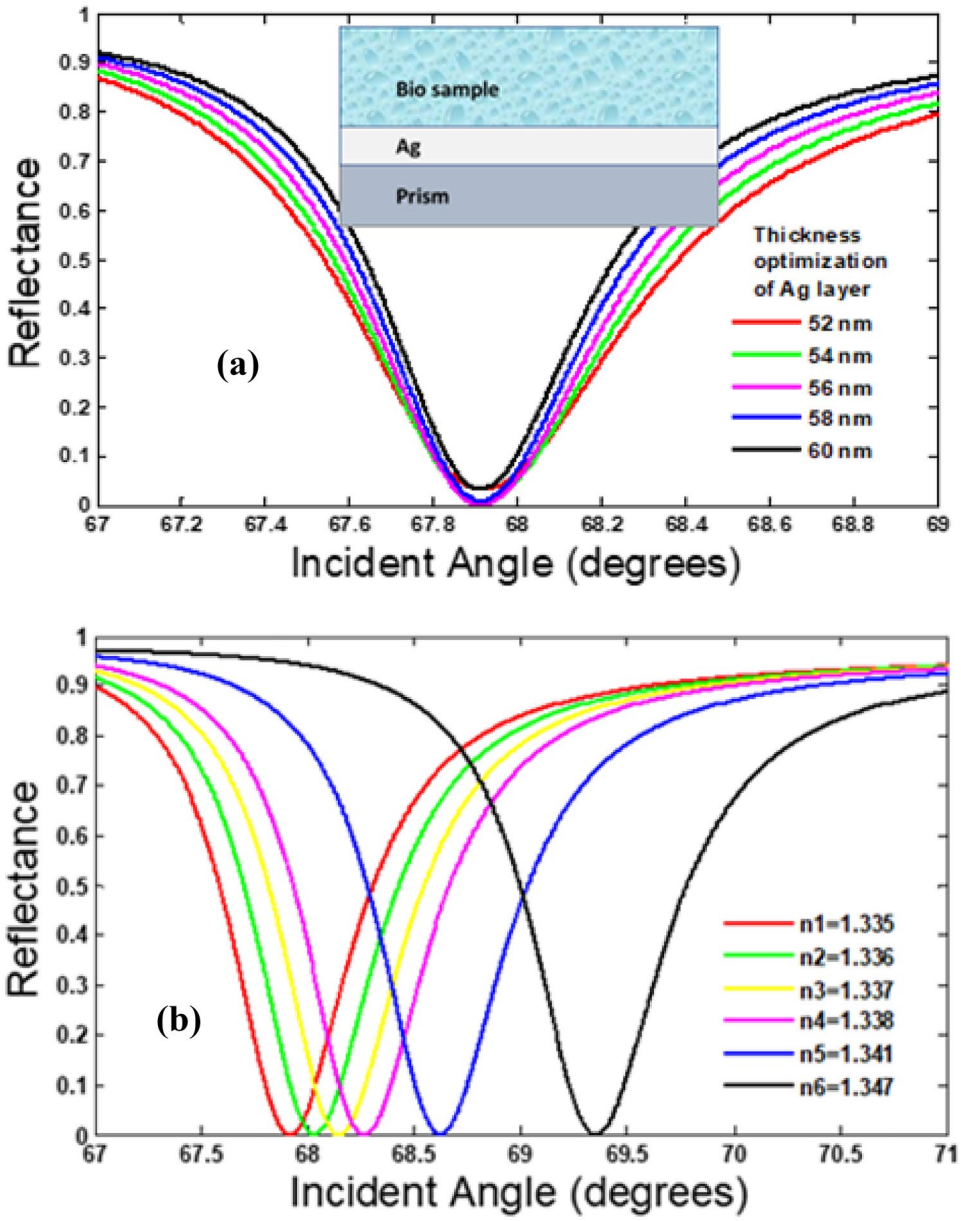

Fig. 3 **a**. Thickness optimization reflectance curve for Ag layer **b**. SPR curves for urine sample with corresponding angle shift for Ag based Structure

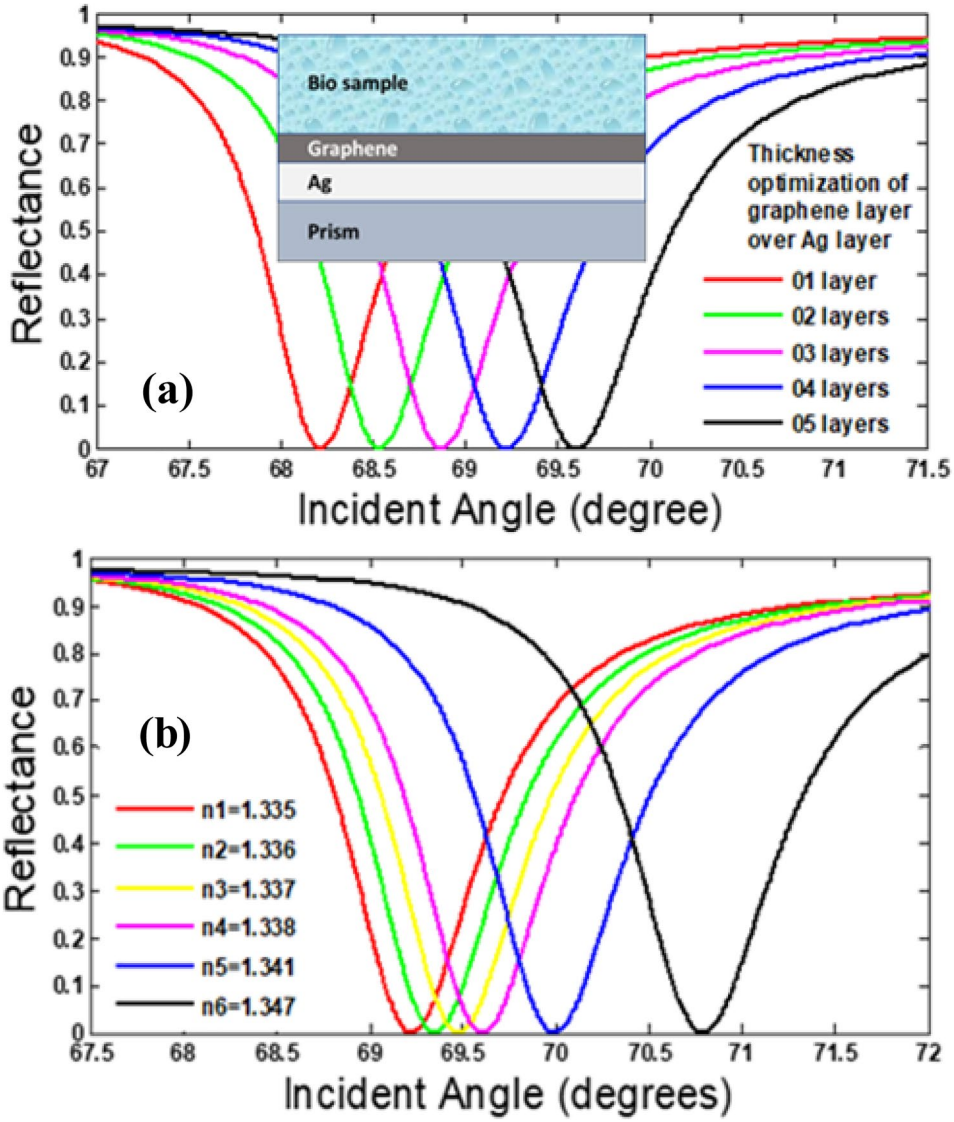

Fig. 4 **a** Thickness optimization reflectance curves for graphene layers over Ag layers. **b**. SPR curves for urine sample with corresponding angle shift for Ag/graphene-based structure

0.00193 at an angle of 67.9°. Applying a biosample of different glucose concentrations to this, the sensitivity is found as 105 °/RIU, as shown in Fig. 3b.

Further, the Ag layer is coated with graphene, which also protects Ag from oxidation. The thickness of a graphene layer is of 0.34 nm. Figure 4a shows the resonance angle shift with respect to the R_{min} with increasing the number of graphene layers (say, $X = 1$ to 5). It can be seen that all considered layers show almost identical reflectance with different resonant angles. Though, any one of these angles can be considered, however, simulations show that (as shown later), a combination of four layers of graphene is the most suitable one for further investigation, along with the next considered material layer. Figure 4b shows the reflectance plot for the present configuration with different urine-glucose concentrations. It can be seen that, with 4 layers of graphene sheets, the present structure has achieved a R_{min} of 0.00019 (at $\theta = 69.2°$) and a sensitivity of 144.44°/RIU.

Additionally, we apply tungusten disulfide (WS_2) layers on top of the graphene layers to improve the performance of the proposed biosensor. For the investigation, we have used

Table 2 Sensitivity of Prism/Ag/ Graphene/WS_2/ biosample for different number of graphene and WS_2 layers

Graphene (X)	Sensitivity (S) in °/RIU for WS_2 Layer (Y)				
	Y = 0	Y = 1	Y = 2	Y = 3	Y = 4
0	105	--	--	--	--
1	105	144.44	183.33	161.11	205.55
2	--	111.11	188.88	161.11	216.66
3	--	116.66	122.22	161.11	255.55
4	--	150	161.11	172.22	288.86

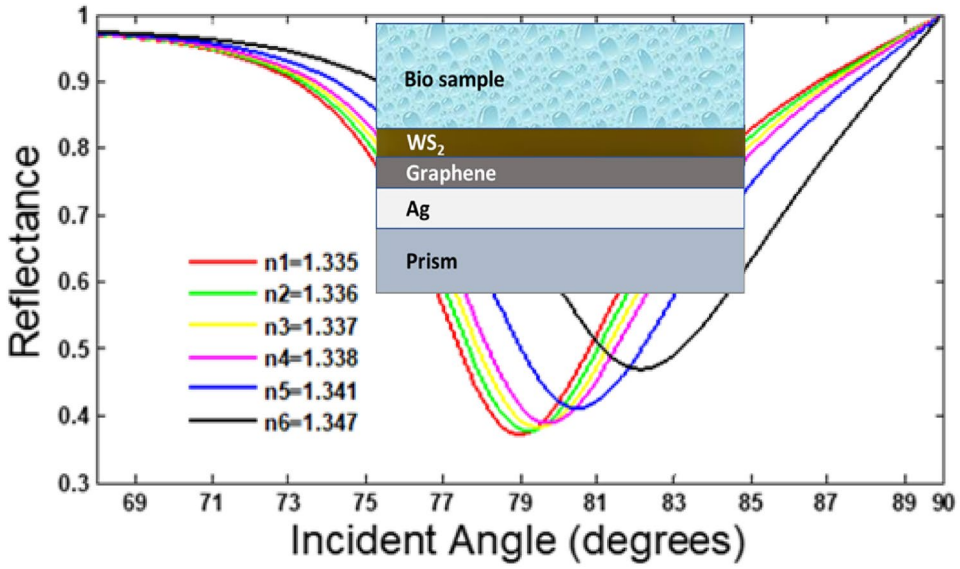

Fig. 5 SPR curves for urine sample with corresponding angle shift for Ag/graphene/WS_2 based structure

WS_2 layers of $Y=1$, 2, 3, 4, and 5. Simulations show that sensitivity of the structure increases with an increase in the WS_2 layer and reaches its maximum at $Y=4$.

Table 2 shows the corresponding sensitivity of the present structure with increasing number of graphene and WS_2 layers. It can be seen that; the sensor shows improved sensitivity with four layer of graphene and the sensitivity further increases with increase in the WS_2 layer. The corresponding sensitivity with 1–4 number of WS_2 layer are 150°/RIU, 161.11°/RIU, 172.22°/RIU, and 288.86°/RIU, respectively. However, simulation also shows that a further increment in WS_2 layer ($Y=5$) reduces sensitivity to 111.11°/RIU. Based on the above analysis, the present structure can be optimized as a prism/Ag (56 nm)/graphene (4×0.34 nm)/WS_2 (4×0.8 nm)/biosample. Figure 5 shows the reflectance curves and corresponding shift in angle for the optimised structure.

For urine samples of 0–15 mg/dl (normal person) to 0.625 gm/dl (diabetic person), the difference in refractive index is 0.001 and the corresponding change in resonance angle $\Delta\theta_{res}$ =0.26829° (Fig. 5) i.e., from 82.34148° to 82.61077°. This shows that, the proposed biosensor is capable of showing a significant angle shift of 0.26929° with a minute change of 0.001 in the analyte refractive index. Similarly, the change in refractive index and corresponding change in angle shift for all the urine samples are given in Table 3.

Figure 6 depicts the electric field plot of the proposed silver-based structure. It can be seen from both Fig. 6a, b that, the proposed structure shows a prominent field pattern with sharp spike at the WS_2-biosample interface, hence supporting its highly sensitive nature.

Investigation has also been carried out by interchanging the order of graphene and WS_2 layers over the Ag layer to check the performance of the proposed biosensor. Firstly, the Prism/Ag/WS_2/biosample configuration is considered, and the R_{min} for different WS_2 layers are shown in Fig. 7. It can be seen that, the structure shows the lowest R_{min} value of 0.03989 at an angle 69.06548° for monolayer of WS_2. Considering this, the reflectance for different urine samples is plotted in Fig. 7. Based on the figure, the sensitivity of the considered structure is calculated to be 111.11°/RIU. Sensitivity of the present structure without and with increasing number of graphene layer over increasing number of WS_2 layer are given in Table 4. While increasing the number of WS_2 layers obtained sensitivities are 150°/RIU, 188.88°/RIU, 205°/

Table 3 Resonance angle shift and reflectance for the proposed biosensor (Prism/Ag(56 nm)/graphene(4×0.34)/WS_2(4×0.80 nm)/urine)

Glucose Level (g/dl)	Refractive Index	Change in Refractive Index	Incident angle (degrees)	Change in Incident angle	Reflectance
0	1.335	Reference	82.34148	Reference	0.48283
0.625	1.336	0.001	82.61077	0.26929	0.49663
1.25	1.337	0.001	82.87548	0.26471	0.51147
2.5	1.338	0.001	83.13331	0.25783	0.52742
5	1.341	0.003	83.83576	0.70245	0.58182
10	1.347	0.006	84.68374	0.84798	0.70873

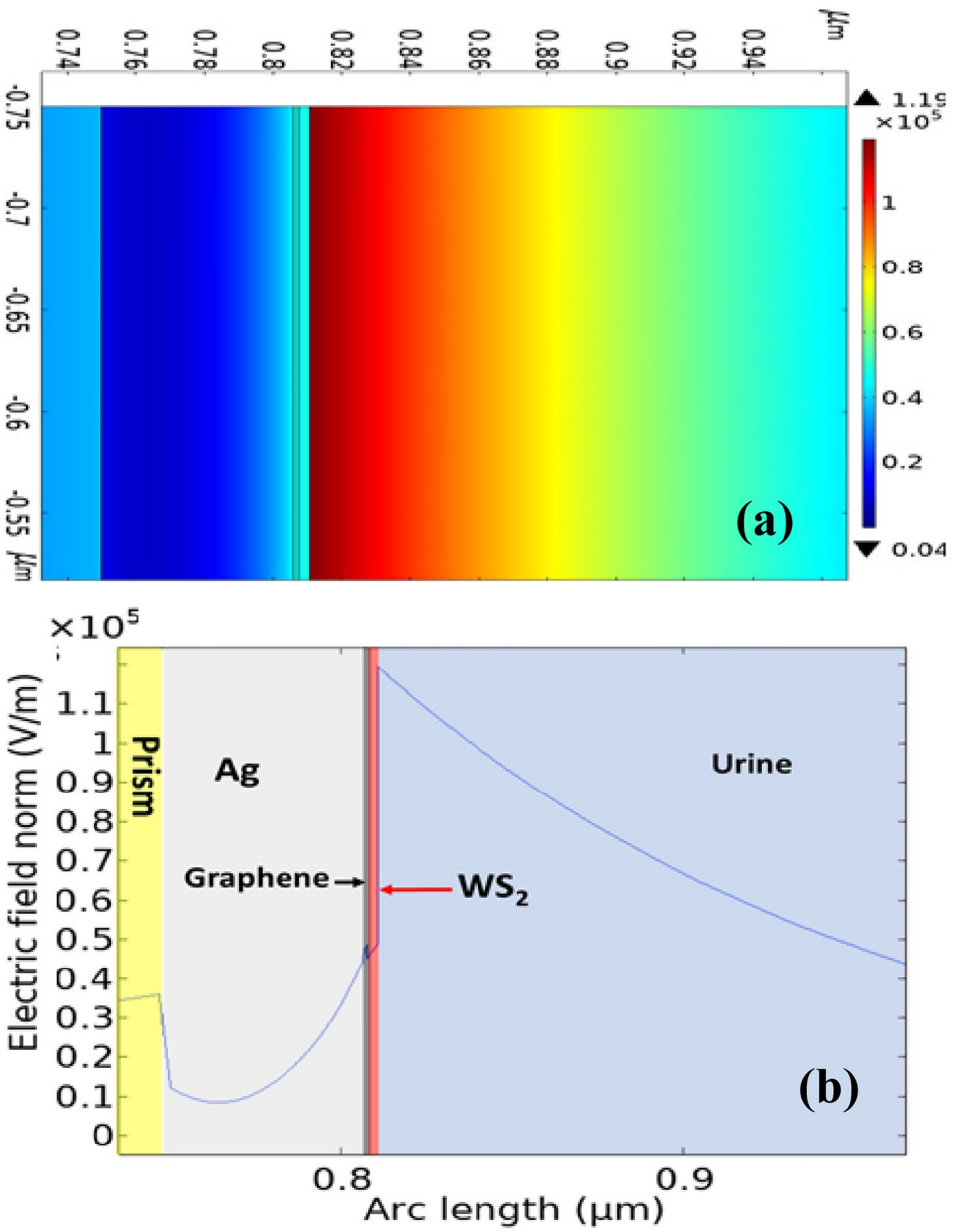

Fig. 6 **a** Electric field profile and **b** corresponding line plot for magnitude of electric field distribution for proposed prism/Ag/graphene/WS_2 structure ($\Delta n = 0.001$)

RIU and 255°/RIU for the layers 2, 3, 4 and 5 respectively. Further increasing the 6 layers of WS_2, sensitivity drops to 150 °/RIU. A comparison of the proposed work with other similar reported work is given in Table 5.

Further, simulation has been done by interchanging the graphene layers and WS_2 layers. Different combination of WS_2 and graphene layers has been investigated. Respective sensitives have been calculated and shown in the Table 4. The best obtained sensitivity is for the 4 layers of graphene over the 4 layers of WS_2 is 261.11 °/RIU.

Table 4 Sensitivity of the structure Prism/Ag/ WS_2/ Graphene/ biosample for different number of WS_2 and graphene layers

WS_2 Layer (Y)	Sensitivity (S) in °/RIU for Graphene layer (X)				
	X = 0	X = 1	X = 2	X = 3	X = 4
1	111.11	144.44	144.44	116.66	177.77
2	--	150	116.66	188.88	122.22
3	--	188.88	161.11	200	205.55
4	--	205.55	211.11	222.22	261.11

Reflectance curve and corresponding angle shift for this structure has been shown in Fig. 7 (with graphene in Fig. 8), and are lesser as compared to the proposed optimized structure based on 4 layers of WS_2 over 4 layers of graphene.

The above discussion can be summarized by saying that, gold-free SPR sensors can be developed using graphene and WS_2, which also shows far better performance than the conventional gold based SPR sensors. The proposed configuration can be useful for design of low cost and efficient SPR sensors which can be an easy access to a wide range of customers.

Fabrication Feasibility

The fabrication feasibility of the device structure is discussed here. Firstly, an Ag layer is deposited over the base of the BK7 prism using the physical vapour deposition (PVD) technique [32]. The graphene layer can also be deposited using chemical vapour deposition (CVD) technique [33]. Growth of WS_2 on graphene sometimes need very high temperature. However, growth of WS_2 on graphene at low temperatures can be achieved through sulfurization of a tungsten precursor on graphene or by plasma-enhanced atomic layer deposition (PEALD) technique using $W(CO)_6$ and H_2S plasma at a relatively low temperature of 350 °C [15]. The resulting WS_2 layer can be characterized using techniques such as scanning electron microscopy (SEM), atomic force microscopy (AFM), Raman spectroscopy, and X-ray photoelectron spectroscopy (XPS) to assess the quality, thickness, and structural properties of the WS_2 layer. This setup is considered for sensing operation. The urine sample can now be applied to the WS_2 layer for performing the sensing operation.

The sensor structure is now placed on a rotary base, and a goniometer is employed to set the resonance angle. Then a monochromatic p-polarised light is shined on one side of the prism, and the reflected light at the other side is detected using a photo detector. The obtained reflection spectra are used to determine the concentration of biomarkers in the biosample.

The proposed configuration can also be realized using optical fiber configuration, which work in a similar way as the prism-based configuration [34, 35]. Both the configurations have their own merits and demerits depending on the fabrication process and application. However, we choose the later one to take certain benefits (not absolute) while realization of the sensor in future.

The main difference between both the optical fiber and prism-based configuration is that the former one relies on evanescent field interactions with the surrounding medium, while the later one provides stronger interaction between the light and the sample. This often makes the prism-based configuration more sensitive with a large measurement range. Additionally, fiber optic plasmonic sensors require more complex and delicate fabrication and alignment processes compared to prism-based sensors, which requires precise control to achieve optimal sensing performance.

Table 5 Comparison of Proposed Biosensor with existing work

Ref.	Year	Sensitivity enhancement strategy	λ in nm	Sensitivity (°/RIU)
This Work	2023	BK7-Ag-graphene- WS_2 Biosample	633	288.86
[23]	2023	BK7/MgO/Ag/BP	633	234
[24]	2022	BK7/Ag/MXene/Ag/ZnO/graphene	633	161
[25]	2021	BK7/Au/WSe2/PtSe2/BP	633	200
[26]	2021	SF10/Au/a-SnSe2/Phosphorene	633	96.4
[27]	2020	BK7/Au/WSe2/Graphene	633	178.8
[28]	2020	SF11/Au/MoS2/WS2/ WSe2	633	142
[29]	2020	SF11/Au/MoS2/Graphene	633	130
[17]	2020	BK7/ZnO/Ag/BaTiO3/WS2	633	180
[30]	2019	BK7/Au/WS2/Au/MXene	633	198
[18]	2019	Prism/Au/SnSe/Graphene	633	94.29
[31]	2019	Prism/Ag/Franckite/Graphene	633	196.00

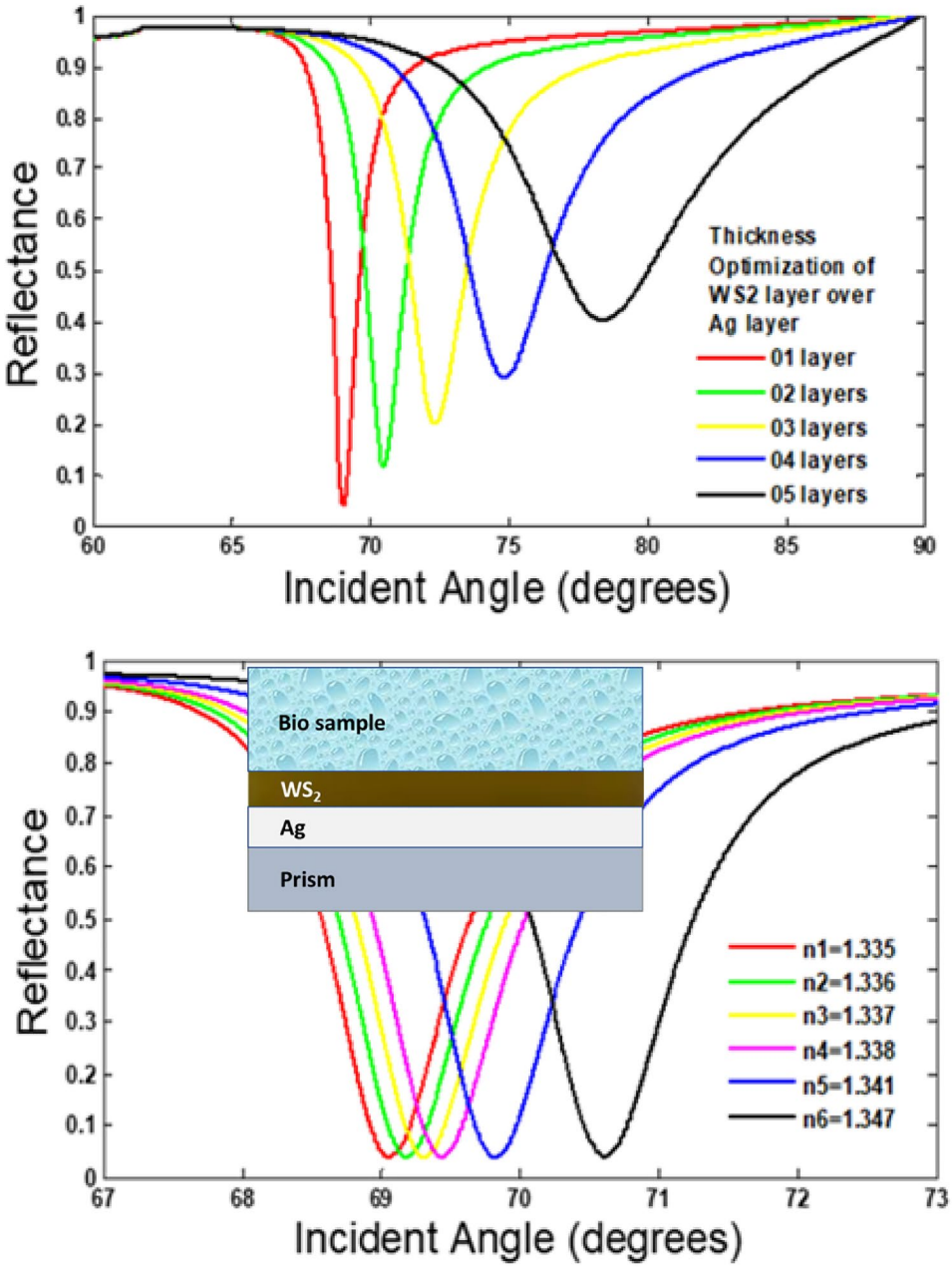

Fig. 7 Thickness optimization reflectance curve for WS2 layer over Ag layer and SPR curves for urine sample with corresponding angle shift for Ag/WS2 based Structure

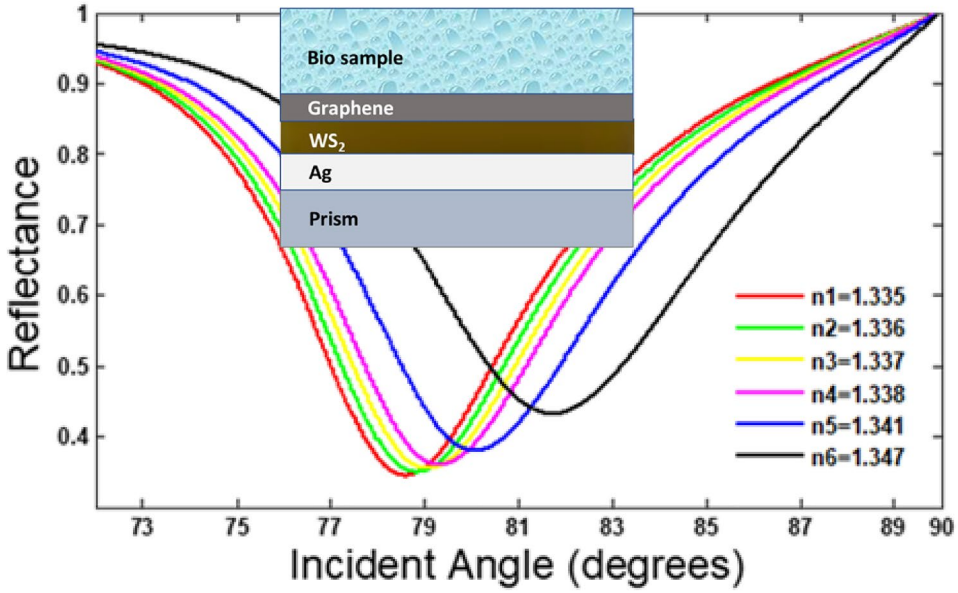

Fig. 8 SPR curves for urine sample with corresponding angle shift for Ag/ WS_2/ graphene-based structure

Conclusions

In this study, we propose a gold-free, graphene and WS_2-based SPR biosensor for low cost and efficient urine-glucose detection. Simulations demonstrate that a silver-based SPR biosensor with four layers of graphene and four layers of WS_2 has superior sensitivity and field enhancement than a gold-based SPR biosensor. A variety of case studies gave rise to an optimum configuration with thickness of Ag (56 nm), Graphene (1.36 nm), and WS_2 (3.2 nm), and it exhibits a sensitivity of 288.86 °/RIU and a Figure of Merit of 88.89 °/RIU. By removing the need of Au, the suggested structure may be effectively used for detecting glucose concentrations in urine, as shown by a significant shift in the resonance angle in SPR curves. The extension of the proposed design could be done for efficient sensing of other biomarkers for detection of respective diseases. Following a similar approach, optimization of the structure can also be done for analytes other than biomarkers to design low-cost sensors for a variety of applications such as chemical, gas, and heavy metal detections.

Acknowledgements The authors thank I-STEM Govt. of India for providing the simulation platform. Archana Yadav acknowledges to Integral University, Lucknow, for providing manuscript communication number IU/R&D/2023-MCN0002056.

Author Contributions Archana Yadav formulated the problem statement, giving the theoretical background and mathematical modeling for the SPR biosensor. Madhusudan Mishra worked on methodology and simulation of the design. Madhusudan Mishra, Sukanta K.T ripathy, and Anil Kumar worked towards the validating the design and finalized the design results. O.P. Singh and Preeta Sharan worked towards the manuscript formatting, and finalizing the manuscript. All authors contributed to write the manuscript and finalized the manuscript for submission.

Data Availability Necessary details have been provided in the article.

Declarations

Ethics Approval Not Applicable.

Consent to Participate I am willing to participate in the work presented in this manuscript.

Consent for Publication The authors have given their consent to publish this work.

Competing Interests The authors declare no competing interests.

Conflicts of interest The authors declare no conflict of interest.

References

1. Alagdar M, Yousif B, Areed NF, Elzalabani M (2020) Improved the quality factor and sensitivity of a surface plasmon resonance sensor with transition metal dichalcogenide 2D nanomaterials. J Nanoparticle Res 22(7):1–13. https://doi.org/10.1007/S11051-020-04872-0/TABLES/2
2. Li L, Huang T, Zhao X, Wu X, Cheng Z (2018) Highly sensitive SPR sensor based on hybrid coupling between plasmon and photonic mode. IEEE Photonics Technol Lett 30(15):1364–1367. https://doi.org/10.1109/LPT.2018.2847907
3. Homola J, Yee SS, Gauglitz G (1999) Surface plasmon resonance sensors: review. Sens Actuators B Chem 54(1):3–15. https://doi.org/10.1016/S0925-4005(98)00321-9
4. Singh S et al (2020) 2D nanomaterial-based surface plasmon resonance sensors for biosensing applications. Micromachines 11(8):1–28. https://doi.org/10.3390/mi11080779
5. Kumar S et al (2022) Plasmon-based Tapered-in-tapered fiber structure for p-cresol detection: from human healthcare to aquaculture application. IEEE Sens J 1–1. https://doi.org/10.1109/JSEN.2022.3200055

6. Nurrohman DT, Chiu N-F (2020) Surface Plasmon Resonance Biosensor performance analysis on 2D material based on Graphene and Transition Metal Dichalcogenides. ECS J Solid State Sci Technol 9(11):115023. https://doi.org/10.1149/2162-8777/abb419
7. Schutte WJ, De Boer JL, Jellinek F (1987) Crystal structures of tungsten disulfide and diselenide. J Solid State Chem 70(2):207–209. https://doi.org/10.1016/0022-4596(87)90057-0
8. Bui VQ, Pham TT, Le DA, Thi CM, Le HM (2015) A first-principles investigation of various gas (CO, H2O, NO, and O2) absorptions on a WS2 monolayer: stability and electronic properties. J Phys Condens Matter 27(30). https://doi.org/10.1088/0953-8984/27/30/305005
9. Johnson PB, Christy RW (1972) Optical constants of the noble metals. Phys Rev B 6(12):4370. https://doi.org/10.1103/PhysRevB.6.4370
10. Alagdar M, Yousif B, Areed NF, Elzalabani M (2020) Highly sensitive fiber optic surface plasmon resonance sensor employing 2D nanomaterials. Appl Phys A Mater Sci Process 126(7):1–16. https://doi.org/10.1007/S00339-020-03712-1/TABLES/2
11. Sharma N, Joy A, Mishra AK, Verma RK (2015) Fuchs Sondheimer-Drude Lorentz model and drude model in the study of SPR based optical sensors: a theoretical study. Opt Commun 357:120–126. https://doi.org/10.1016/j.optcom.2015.08.092
12. McPeak KM et al (2015) Plasmonic films can easily be better: rules and recipes. ACS Photonics 2(3):326–333. https://doi.org/10.1021/ph5004237
13. Loh TAJ, Chua DHC, Wee ATS (2015) One-step Synthesis of Few-layer WS2 by Pulsed Laser Deposition. Sci Rep 5(November):1–9. https://doi.org/10.1038/srep18116
14. Ouyang Q et al (2016) Sensitivity enhancement of transition metal dichalcogenides/silicon nanostructure-based surface plasmon resonance biosensor. Sci Rep 6(1):1–13. https://doi.org/10.1038/srep28190
15. Yeo S et al (2018) Low-temperature direct synthesis of high quality WS 2 thin films by plasma-enhanced atomic layer deposition for energy related applications. Appl Surf Sci 459:596–605. https://doi.org/10.1016/j.apsusc.2018.07.210
16. Sharma P, Sharan P (2015) Design of photonic crystal-based biosensor for detection of glucose concentration in urine. IEEE Sens J 15(2):1035–1042. https://doi.org/10.1109/JSEN.2014.2359799
17. Kumar A, Yadav AK, Kushwaha AS, Srivastava SK (2020) A comparative study among WS2, MoS2 and graphene based surface plasmon resonance (SPR) sensor. Sens Actuators Rep 2(1):100015. https://doi.org/10.1016/J.SNR.2020.100015
18. Nisha A, Maheswari P, Anbarasan PM, Rajesh KB, Jaroszewicz Z (2019) Sensitivity enhancement of surface plasmon resonance sensor with 2D material covered noble and magnetic material (ni). Opt Quantum Electron 51(1). https://doi.org/10.1007/S11082-018-1726-3
19. Yamamoto M (2015) Surface Plasmon Resonance (SPR) theory: Tutorial Surface Plasmon Resonance (SPR) theory : Tutorial. no June. https://doi.org/10.5189/revpolarography.48.209
20. Shalabney A, Abdulhalim I (2010) Electromagnetic fields distribution in multilayer thin film structures and the origin of sensitivity enhancement in surface plasmon resonance sensors. Sens Actuators Phys 159(1):24–32. https://doi.org/10.1016/j.sna.2010.02.005
21. Raether H (1988) Intro_Contents. Intro_Surface Plasmons on Smooth and Rough Surfaces and on Gratings, p 78
22. Sreekanth KV, Zeng S, Yong KT, Yu T (2013) Sensitivity enhanced biosensor using graphene-based one-dimensional photonic crystal. Sens Actuators B Chem 182:424–428. https://doi.org/10.1016/j.snb.2013.03.039
23. Kumar S, Yadav A, Malomed BA (2023) High performance surface plasmon resonance based sensor using black phosphorus and magnesium oxide adhesion layer. Front Mater 10:1131412. https://doi.org/10.3389/FMATS.2023.1131412/BIBTEX
24. Karki B, Vasudevan B, Uniyal A, Pal A, Srivastava V (2022) Hemoglobin detection in blood samples using a graphene-based surface plasmon resonance biosensor. Optik (Stuttg) 270:169947. https://doi.org/10.1016/J.IJLEO.2022.169947
25. IEEE Xplore Full-Text PDF: https://ieeexplore.ieee.org/stamp/stamp.jsp?arnumber=9658505. Accessed 5 Jul 2023
26. Rikta KA, Anower MS, Rahman MS, Rahman MM (2021) SPR biosensor using SnSe-phosphorene heterostructure. Sens Bio-Sensing Res 33:100442. https://doi.org/10.1016/J.SBSR.2021.100442
27. Nurrohman DT, Chiu NF (2021) A review of Graphene-Based surface Plasmon Resonance and Surface-Enhanced Raman scattering Biosensors: current status and future prospects. Nanomater 11(1):216. https://doi.org/10.3390/NANO11010216
28. Lin Z, Chen S, Lin C (2020) Sensitivity improvement of a Surface Plasmon Resonance Sensor based on two-dimensional materials hybrid structure in visible region: a theoretical study. Sens 20(9):2445. https://doi.org/10.3390/S20092445
29. Hossain MB et al (2020) Numerical modeling of MoS2–graphene bilayer-based high-performance surface plasmon resonance sensor: structure optimization for DNA hybridization. 59(10):105105. https://doi.org/10.1117/1.OE.59.10.105105
30. Xu Y, Ang YS, Wu L, Ang LK (2019) High sensitivity surface plasmon resonance sensor based on two-dimensional MXene and transition metal dichalcogenide: a theoretical study. Nanomater 9(2):165. https://doi.org/10.3390/NANO9020165
31. Srivastava A, Prajapati YK (2019) Performance analysis of silicon and blue phosphorene/MoS2 hetero-structure based SPR sensor. Photonic Sens 9(3):284–292. https://doi.org/10.1007/S13320-019-0533-1/METRICS
32. Singh S, Sharma AK, Lohia P, Dwivedi DK, Kumar V, Singh PK (2023) Simulation study of reconfigurable surface plasmon resonance refractive index sensor employing bismuth telluride and MXene nanomaterial for cancer cell detection. Phys Scr 98(2):025813. https://doi.org/10.1088/1402-4896/ACB023
33. Jussila H, Yang H, Granqvist N, Sun Z (2016) Surface plasmon resonance for characterization of large-area atomic-layer graphene film. Optica 3(2):151. https://doi.org/10.1364/optica.3.000151
34. Das P et al (2022) Co3O4Magnetic nanoparticles-coated optical fibers for sensing Sialic Acid. ACS Appl Nano Mater 5(7):8973–8981. https://doi.org/10.1021/ACSANM.2C01172/SUPPL_FILE/AN2C01172_SI_001.PDF
35. Dash SP, Patnaik SK, Tripathy SK (2019) Investigation of a low cost tapered plastic fiber optic biosensor based on manipulation of colloidal gold nanoparticles. Opt Commun 437:388–391. https://doi.org/10.1016/J.OPTCOM.2018.12.088